The total yield of the NAD adducts A–E based on consumed isoniazid is roughly 50% under the conditions shown in Figure 1 (micromolar concentrations of both isoniazid and NAD^+). The efficient formation of the inhibitor **2** in the absence of InhA is, in our opinion, of great importance for an understanding of the mechanism of action of isoniazid. As the concentration of NAD^+ inside *M. tuberculosis* is also in the micromolar range,[15] we propose that inside the bacterium **2** is formed by the fast addition of acyl radical **3** to electron-deficient heterocycles such as NAD^+ and outside the active site of InhA. Considering the low binding affinity of InhA for NAD^+ ($K_I = 4$ mM) and the resulting low concentration of InhA-bound NAD^+,[5] the also conceivable addition of **3** to NAD^+ within the active site of InhA appears rather unlikely. Furthermore, the catalase-peroxidase KatG does not play an active role in the addition of **3** to NAD^+ (although it is required for oxidation of isoniazid), as the yield of isonicotinoyl-NAD adducts as well as the product composition is about the same after oxidation of isoniazid by KatG or Mn^{3+}. The mechanism of action of isoniazid therefore relies on the efficient formation of the isonicotinoyl–NAD adducts by a Minisci reaction as well as the inhibitory potential of **2** (=B/E), whose K_I value is about 100 nM (see above) and therefore about a factor of 100 below the K_M value of InhA for NADH.[5, 12]

The proposed reaction mechanism also allows one to reinterpret the observations that a number of isoniazid-resistant mycobacteria appear to possess a higher ratio of NADH/NAD^+ as the result of defects in NADH-dehydrogenases,[16a] and that overexpression of NAD^+-binding proteins might contribute to isoniazid-resistance.[16b] A lower intracellular concentration of NAD^+ should, according to our mechanism, directly lead to a diminished rate of formation of **2** and therefore to an increased resistance towards isoniazid.

In summary, the demonstrated spontaneous formation of the bioactive form of isoniazid significantly simplifies the proposed mechanism of action of the drug and should be helpful in obtaining a better understanding of the molecular events leading to isoniazid-resistance.

Received: March 16, 1999 [Z13168IE]
German version: *Angew. Chem.* **1999**, *111*, 2724–2727

Keywords: bioorganic chemistry · cofactors · enzyme catalysis · enzyme inhibitors

[1] B. R. Bloom, C. J. L. Murray, *Science* **1992**, *257*, 1055–1064.
[2] a) Y. Zhang, B. Heym, B. Allen, D. Young, S. Cole, *Nature* **1992**, *258*, 591–593; b) K. Johnsson, P. G. Schultz, *J. Am. Chem. Soc.* **1994**, *116*, 7425–7426.
[3] F. G. Winder, P. B. Collins, *J. Gen. Microbiol.* **1970**, *63*, 41–48.
[4] a) A. Banerjee, E. Dubnau, A. Quemard, V. Balasubramanian, K. Sun Um, T. Wilson, D. Collins, G. de Lisle, W. R. Jacobs, Jr., *Science* **1994**, *263*, 227–230; b) K. Mdluli, R. A. Slayedn, Y. Zhu, S. Ramaswamy, X. Pan, D. Mead, D. D. Crane, J. M. Musser, C. E. Barry III, *Science* **1998**, *280*, 1607–1610.
[5] A. Quemard, J. C. Sacchettini, A. Dessen, C. Vilcheze, R. Bittman, W. R. Jacobs Jr., J. S. Blanchard, *Biochemistry* **1995**, *34*, 8235–8241.
[6] K. Johnsson, D. S. King, P. G. Schultz, *J. Am. Chem. Soc.* **1995**, *117*, 5009–5010.
[7] D. A. Rozwarski, G. A. Grant, D. H. R. Barton, W. R. Jacobs, Jr., J. C. Sacchettini, *Science* **1998**, *279*,98–102.
[8] F. Minisci, E. Vismara, F. Fontana, *Heterocycles* **1989**, *28*, 489–519.
[9] Recombinant InhA was purified by using a N-terminal His-tag.[10] For the incubation experiments, InhA (5.4 μM) was incubated with horseradish peroxidase (44 μM), isoniazid (250 μM), $MnCl_2$ (7.5 μM) and either NAD^+ or NADH (each 47 μM) at pH 7.5 (50 mM Na_2HPO_4) and 25 °C. The InhA activity was monitored by using a NADH-based assay.[6] After the activity dropped below 10% of the value at t_0, the sample was dialyzed for 12 h at 4 °C in a microdialysis system (GibcoBRL; *Cut-off* of the dialysis membrane: 12–14 kD) against 100 mM triethylammonium acetate, pH 7. MALDI-TOF spectra were recorded by using a RP Biospectrometry Voyager DE; sinapinic acid, 2,5-dihydroxybenzoic acid, or 2-amino-5-nitropyridine were used as a matrix.
[10] M. Wilming, Diploma thesis, Universität Bochum, **1998**.
[11] HPLC analysis was performed on a Merck LiChroCART 250–4 Purospher RP-18e (5 μm) using a linear gradient from NH_4OAc (75 mM) to acetonitrile. UV spectra of the peaks were recorded using a diode-array detector (Kontron 440).
[12] The K_I value of product B/E was determined by using 2-*trans*-octenoyl-CoA and NADH as substrates at pH 7.5 (100 mM Na_2HPO_4) and 25 °C. At fixed concentrations of NADH and 2-*trans*-octenoyl-CoA the concentration of B/E was varied.
[13] Y. Pocker, J. E. Meany, *J. Am. Chem. Soc.* **1967**, *89*, 631–636.
[14] (4-^{2}H)-NAD^+ was synthesized according to the procedure of Charlton et al.: P. A. Charlton, D. W. Young, B. Birdsall, J. Feeny, G. C. K. Roberts, *J. Chem. Soc. Perkin Trans. 1* **1985**, 1349–1353.
[15] K. P. Gopinathan, M. Sirsi, T. Ramakrishnan, *Biochem. J.* **1963**, *87*, 444–448.
[16] a) L. Miesel, T. R. Weisbrod, J. A. Marcinkeviciene, R. Bittman, W. R. Jacobs Jr., *J. Bacteriol.* **1998**, *180*, 2459–2467; b) P. Chen, W. R. Bishai, *Infect. Immun.* **1998**, *66*, 5099–5106.

A Microporous Lanthanide–Organic Framework**

Theresa M. Reineke, Mohamed Eddaoudi, M. O'Keeffe, and Omar M. Yaghi*

The recent upsurge of reports on open metal–organic frameworks has provided compelling evidence for the ability to design and produce structures with unusual pore shape, size, composition, and function.[1] To realize the potential of these materials in host–guest recognition, separation, and catalysis, it is essential that their frameworks exhibit perma-

[*] Prof. O. M. Yaghi,[+] T. M. Reineke,[+] Dr. M. Eddaoudi,[+]
Prof. M. O'Keeffe
Materials Design and Discovery Group
Department of Chemistry and Biochemistry
Arizona State University, Box 871604, Tempe, AZ 85287 (USA)
[+] New address:
Department of Chemistry
University of Michigan
Ann Arbor, MI 48109-1055 (USA)
Fax: (+1) 734-763-2307
E-mail: oyaghi@umich.edu

[**] The financial support of this work by the National Science Foundation (Grant CHE-9522303) and Department of Energy (Division of Chemical Sciences, Office of Basic Energy Sciences, Grant DE-FG03-98ER14903), and the crystallographic work provided by Dr. Fred Hollander (University of California-Berkeley) are gratefully acknowledged.

  1433-7851/99/3817-2590 $ 17.50+.50/0

nent microporosity even in the absence of guests, an aspect that is routinely considered for zeolites[2] but has remained largely unexplored for the analogous metal–organic materials.[3] In attempting to address this issue, we aimed at coupling our interest in designing new frameworks with the desire to achieve stable microporous structures. Here we report the synthesis and structure of $Tb(bdc)NO_3 \cdot 2DMF$ (bdc = 1,4-benzenedicarboxylate; DMF = *N*,*N*-dimethylformamide) and show that its desolvated derivative $Tb(bdc)NO_3$ has a stable zeolite-like framework that is capable of reversible molecular sorption and of maintaining microporosity in the absence of included guests.

Previous studies on the copolymerization of Zn^{II} with BDC have shown that stable frameworks can be produced.[3d, 4] This was attributed to the bis-bidentate functionality of BDC and its tendency to form large, tightly bound metal carboxylate cluster aggregates that ultimately act as building blocks in the crystal structure. We sought to extend this strategy to the pursuit of lanthanide–organic open frameworks, which remain virtually unknown, despite the established role of lanthanide compounds sensor technology.[5]

Deprotonation of the acid form of BDC (H_2BDC) with pyridine followed by its copolymerization with Tb^{III} in methanol/DMF at room temperature gave a crystalline colorless solid, which was formulated as $Tb(bdc)NO_3 \cdot 2DMF$ on the basis of elemental analysis and single-crystal X-ray diffraction.[6, 7] Complete deprotonation of BDC was confirmed by the absence of any strong absorption bands due to protonated carboxyl groups (1715–1680 cm^{-1}) in the FT-IR spectrum.[6] This material is stable in air and is insoluble in common organic solvents such as methanol, ethanol, acetonitrile, acetone, and DMF.

The single-crystal structure analysis revealed an extended Tb–BDC framework with two crystallographically distinct Tb atoms, BDC units, nitrate ions, and four DMF ligands. The two Tb atoms are each coordinated by eight oxygen atoms: One each from four carboxylate groups of different BDC ligands, two from a nitrate anion, and one from each of two DMF molecules (Figure 1). The framework is composed only of Tb and BDC, whereby each carboxylate moiety bridges two terbium atoms in a bis-monodentate fashion to form chains along the *c* axis (Figure 2a). These chains are cross-linked by

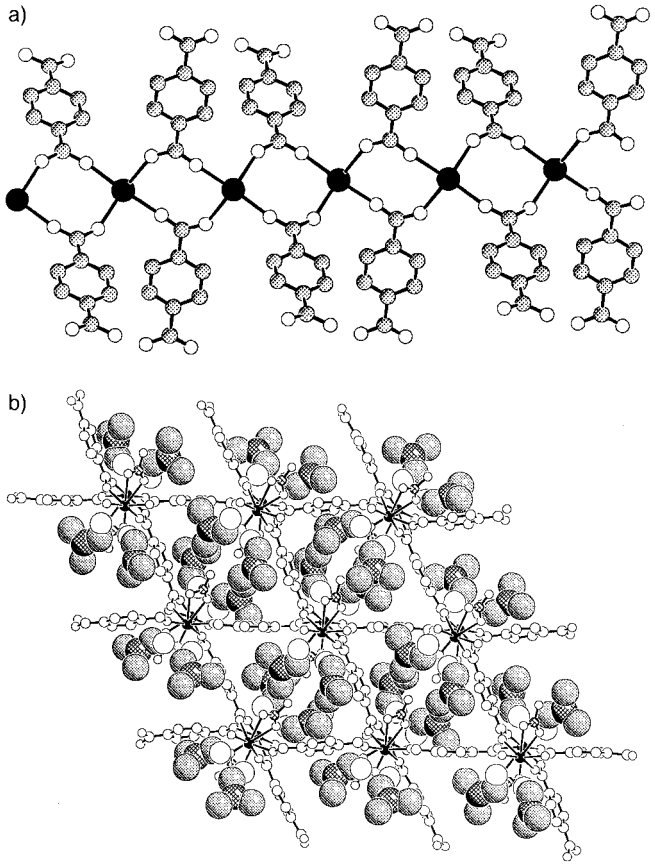

Figure 2. a) Tb–BDC chains shown perpendicular to the *c* axis. b) A projection along the *c* axis with DMF shown in space-filling (C, shaded; N, cross-hatched; O, open) and the Tb–BDC–NO_3 framework as ball-and-stick (Tb, filled; N, cross-hatched; C and O, open) representations. Hydrogen atoms are omitted for clarity.

BDC to form a three-dimensional network (Figure 2b) in which the nitrate anions and DMF molecules point into the channels. The topology of the structure is best described in terms of a simple (3,4)-connected net derived from the 4-connected net of the PtS structure (Figure 3a and b). In this case, each of the planar 4-connected vertices (filled circles) are split into pairs of 3-connected vertices that share a common link.[8] As shown in Figure 3c, the 4-connected

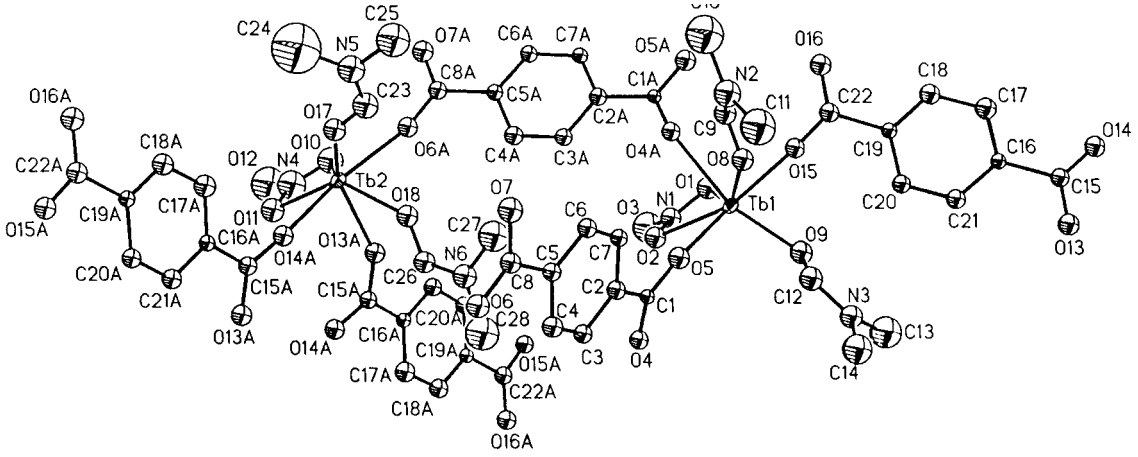

Figure 1. The asymmetric unit of crystalline $Tb(bdc)NO_3 \cdot 2DMF$; atoms labeled by the letter A are related by symmetry to those without such designation.

  1433-7851/99/3817-2591 $ 17.50+.50/0

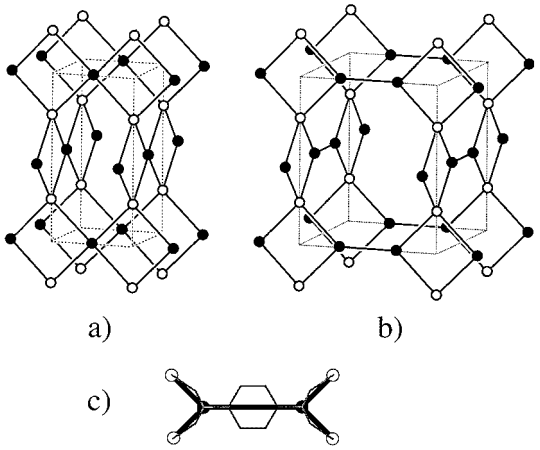

Figure 3. a) The 4-connected net of PtS (S, open; Pt, filled). b) The (3,4)-connected net of $Tb(bdc)NO_3 \cdot 2DMF$ that is derived from (a) by converting the planar 4-connected vertices (filled) to pairs of 3-connected vertices. c) Schematic identification of the atoms in the crystal structure of $Tb(bdc)NO_3 \cdot 2DMF$ with net vertices; open circles are Tb atoms [4-connected vertices in (b)] and filled circles are carboxylate C atoms of BDC [3-connected vertices in (b)]; the benzene ring of BDC is superimposed on the link between 3-connected vertices.

vertices are the Tb atoms which are connected through −O− links to the carboxylate C atoms of BDC (the 3-connected vertices); these are in turn joined in pairs by $-C_6H_4-$ links. In its highest symmetry form the network is tetragonal, space group $P4_2/mmc$, but the symmetry is lower ($P2_1/c$) in the actual crystal structure.

To create an open framework with accessible voids, we examined the possibility of removing the DMF ligands by means of a thermogravimetric (TG) study. A sample of the as-synthesized material (46.87 mg) showed an onset of weight loss at 120°C that terminated at 223°C with 27.1 % total weight loss, which is equivalent to the removal of 1.97 DMF molecules per formula unit (calculated: 27.5 %). The FT-IR spectrum of the remaining solid $Tb(bdc)NO_3$[9] shows similar absorption bands to those of the original solid, albeit with minor differences due to the removal of DMF. Its X-ray powder diffraction pattern was significantly broadened with only two discernible diffraction lines; this indicates a degradation of long-range order. However, the fact that $Tb(bdc)NO_3$ did not show any weight loss up to 320°C suggested the presence of a stable framework material. Resorption of DMF into the solvent-free material resulted in regeneration of the most prominent diffraction lines of the as-synthesized material.

To determine the microporosity of $Tb(bdc)NO_3$, the gas sorption isotherm was measured. Initially, we confirmed the loss of DMF from the original solid by placing a sample of $Tb(bdc)NO_3 \cdot 2DMF$ (151.50 mg) in an electromicrogravimetric balance (CAHN 1000) setup at room temperature under vacuum (5×10^{-5} Torr). Then the loss of DMF was monitored by heating to 135 and 185°C at 0.15 K min^{-1}. The total weight losses of 18.68 (1.35 DMF) and 26.97 % (1.97 DMF), respectively, confirm the TG results. At this point, carbon dioxide (UHP grade) was introduced into the sample chamber containing the completely evacuated sample, and the weight changes were monitored at different pressure intervals at 195 K. When no further weight change was observed, a single isotherm point was recorded. A plot of weight sorbed per gram of $Tb(bdc)NO_3$ versus p/p_0 (p_0 = saturation pressure; 780 Torr for CO_2) revealed a reversible type I isotherm (Figure 4), characteristic of a microporous material with

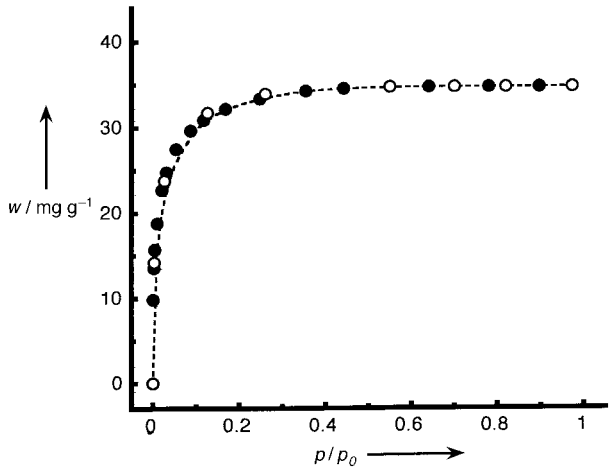

Figure 4. CO_2 sorption (dark circles) and desorption (open circles) isotherm for $Tb(bdc)NO_3$ plotted with sorbed amount w versus relative pressure p/p_0 (p_0 = saturation pressure).

zeolite-like sorption behavior. The pore volume was estimated from this data by using the Dubinin–Raduskhvich equation to be 0.032 cm^3 g^{-1}, which is comparable to that of common zeolites.[2a] Applying the same technique at room temperature for the vapor sorption, we found that dichloromethane (4 Å kinetic diameter) is readily sorbed into the pores of $Tb(bdc)NO_3$ with a type I isotherm. However, sorption of cyclohexane was not observed due to its larger size (6 Å kinetic diameter).[2]

The dissociation and removal of DMF from the channels means that terbium becomes coordinatively unsaturated in the resulting porous solid. Exploring the chemistry of such Lewis acid sites may reveal their potential use in sensors or as catalysts for organic transformations. On studying the solution stability of the porous framework, we observed that immersion of the evacuated solid in water results in its quantitative and irreversible conversion to another recently reported porous solid, namely, $Tb_2(bdc)_3 \cdot 4H_2O$.[5a] Nevertheless, $Tb(bdc)NO_3$ appears to be unaffected by organic solvents, and this allowed allowed the study of its inclusion chemistry.

The solution sorption isotherms for methanol, ethanol, and isopropyl alcohol are shown in Figure 5. A known amount of the evacuated solid (30–40 mg) was immersed in a solution in toluene containing a specific amount of a potential guest (0.10–0.90 M). The change in guest concentration was then measured by gas chromatography with a thermal conductivity detector. Each equilibrium point was obtained by monitoring the change in guest concentration with time until no further change was observed.[10] The sorption process was successfully modeled with a 1:1 complex as suggested by the Langmuir isotherm equation (assuming equivalent available sites), and all compounds showed good agreement to the model with high nonlinear regression parameters (typically 0.99). The

  1433-7851/99/3817-2592 $ 17.50+.50/0

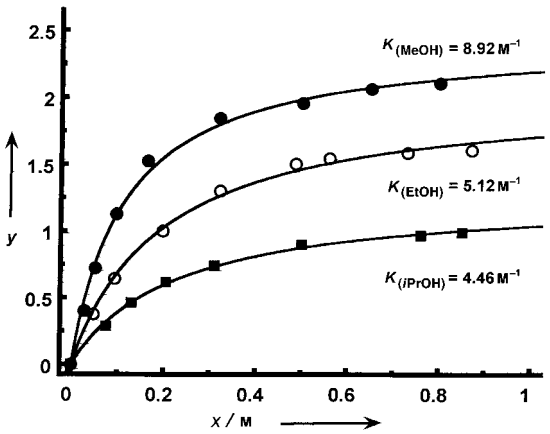

Figure 5. Room-temperature isotherms for the sorption of liquid alcohols by Tb(bdc)NO_3. Molar ratio of guest to Tb(BDC)NO_3 (y) versus equilibrium concentration of guest (x).

results show that the number of molecules sorbed per formula unit decreases as the size of the guest increases, and a similar trend is observed for the association equilibrium constant K (Figure 5). Both of these parameters indicate a size- and shape-dependent inclusion process.

This study demonstrates that lanthanide carboxylate open frameworks can have sufficient stability to support zeolite-like microporosity. Current studies are focused on exploring the accessibility of the Lewis acid metal sites within the channels and the design of analogous frameworks with larger pores.

Experimental Section

Tb(bdc)$NO_3\cdot 2$DMF: 1,4-benzenedicarboxylic acid (H_2BDC) (0.050 g, 0.30 mmol) and terbium(III) nitrate pentahydrate (0.131 g, 0.30 mmol) were placed in a small vial and dissolved in a mixture of methanol (3 mL) and DMF (3 mL) with mild heating. The vial was then placed in a larger vial containing pyridine (4 mL), which was sealed and left undisturbed for 5 d at room temperature. The resulting colorless block-shaped crystals were collected by filtration, washed with methanol (3×10 mL), and air dried to give Tb(bdc)$NO_3\cdot 2$DMF (0.12 g, 73% yield). The isostructural europium analogue was prepared by a similar procedure from europium(III) nitrate pentahydrate.

Received: March 1, 1999 [Z13092IE]
German version: *Angew. Chem.* **1999**, *111*, 2712 – 2716

Keywords: host – guest chemistry · lanthanides · microporosity · zeolite anlogues

[1] a) D. M. L. Goodgame, D. A. Grachvogel, D. J. Williams, *Angew. Chem.* **1999**, *111*, 217; *Angew. Chem. Int. Ed.* **1999**, *38*, 153; b) O. M. Yaghi, H. Li, C. Davis, D. Richardson, T. L. Groy, *Acc. Chem. Res.* **1998**, *31*, 874; c) J. Lu, T. Paliwala, S. C. Lim, C. Yu, T. Niu, A. J. Jacobson, *Inorg. Chem.* **1997**, *36*, 923; d) C. Janiak, *Angew. Chem.* **1997**, *109*, 1499; *Angew. Chem. Int. Ed. Engl.* **1997**, *36*, 1431; e) P. Losier, M. J. Zaworotko, *Angew. Chem.* **1996**, *108*, 2957; *Angew. Chem. Int. Ed. Engl.* **1996**, *35*, 2779; f) G. B. Gardner, D. Venkataraman, J. S. Moore, S. Lee, *Nature* **1995**, *374*, 792; g) O. Yaghi, G. Li, H. Li, *Nature* **1995**, *378*, 703; h) M. Fujita, Y. J. Kwon, O. Sasaki, K. Yamaguchi, K. Ogura, *J. Am. Chem. Soc.* **1995**, *117*, 7287; i) L. Carlucci, G. Ciani, D. M. Proserpio, A. Sironi, *J. Chem. Soc. Chem. Commun.* **1994**, 2755; j) R. Robson, B. F. Abrahams, S. R. Batteen, R. W. Gable, B. F. Hoskins, J. Liu in *Supramolecular Architecture: Synthetic Control in Thin Films and Solids* (Ed.: T. Bein), American Chemical Society, Washington, DC, **1992**, chap. 19; k) T. Iwamoto in *Inclusion Compounds*, *Vol. 5* (Eds.: J. L. Atwood, J. Davies, D. D. MacNicol), Oxford University Press, New York, **1991**, p. 177.

[2] a) D. W. Breck in *Zeolite Molecular Sieves*, *Structure*, *Chemistry*, *and Use*, Wiley, New York, **1974**; b) S. J. Gregg, K. S. W. Sing, *Adsorption*, *Surface Area*, *Porosity*, 2nd ed., Academic Press, London, **1982**.

[3] a) S. A. Allison, R. M. Barrer, *J. Chem. Soc. A* **1969**, 1717; b) D. Ramprasad, G. P. Pez, B. H. Toby, T. J. Markley, R. M. Pearlstein, *J. Am. Chem. Soc.* **1995**, *117*, 10694; c) M. Kondo, T. Yoshitomi, K. Seki, H. Matsuzaka, S. Kitagawa, *Angew. Chem.* **1997**, *109*, 1844; *Angew. Chem. Int. Ed. Engl.* **1997**, *36*, 1725; d) H. Li, M. Eddaoudi, T. L. Groy, O. M. Yaghi, *J. Am. Chem. Soc.* **1998**, *120*, 8571.

[4] H. Li, C. E. Davis, T. L. Groy, D. G. Kelley, O. M. Yaghi, *J. Am. Chem. Soc.* **1998**, *120*, 2186.

[5] a) T. M. Reineke, M. Eddaoudi, M. Fehr, D. Kelley, O. M. Yaghi, *J. Am. Chem. Soc.* **1998**, *121*, 1999; b) *Lanthanide Probes in Life*, *Chemical and Earth Sciences* (Eds.: J.-C. G. Bünzli, G. R. Choppin), Elsevier, Amsterdam, **1989**.

[6] Elemental analysis (%) calcd for $C_{14}H_{18}O_9N_3$Tb: Tb(bdc)$(NO_3)\cdot$ 2DMF: C 31.65, H 3.42, N 7.91; found: C 31.33, H 3.35, N 7.90. FT-IR (KBr, 2000 – 500 cm^{-1}): $\tilde{\nu}$ = 1702 (m), 1663 (vs), 1630 (s), 1591 (vs), 1512 (w), 1440 (s), 1400 (vs), 1314 (s), 1255 (w), 1110 (m), 1064 (w), 1031 (w), 900 (w), 821 (m), 761 (s), 682 (m), 544 (m), 511 cm^{-1} (s). The europium analogue of this compound was also prepared by an identical procedure and found to have the same composition and structure as the terbium compound. Elemental analysis (%) calcd for $C_{14}H_{18}O_9N_3$Eu: Eu(bdc)$(NO_3)\cdot 2$DMF: C 32.07, H 3.46, N 8.01; found: C 32.26, H 3.26, N 8.02.

[7] An X-ray single-crystal analysis was performed on a colorless polyhedral crystal of Tb(bdc)$NO_3\cdot 2$DMF with approximate dimensions of $0.07\times 0.16\times 0.19$ mm at $-115\pm 1^\circ$C: monoclinic, space group $P2_1/c$, a = 17.5986(1), b = 19.9964(3), c = 10.5454(2) Å, β = 91.283(1)°, V = 3710.09(7) Å^3, Z = 8, ρ_{calcd} = 1.90 g cm^{-3}; $\mu(Mo_{K\alpha})$ = 38.57 mm^{-1}. All measurements were made on a SMART CCD area detector with graphite-monochromated $Mo_{K\alpha}$ radiation. Frames corresponding to an arbitrary hemisphere of data were collected by ω scans of 0.30° counted for a total 10.0 s per frame. Cell constants and an orientation matrix, obtained from a least-square refinement of the measured positions of 7766 reflections in the range $3.00 < 2\theta < 45.00^\circ$ corresponded to a primitive monoclinic cell. Data were integrated by the program SAINT[11] to a maximum 2θ value of 49.5° and corrected for Lorentzian and polarization effects by using XPREP[12]. The data were corrected for absorption by comparison of redundant and equivalent reflections by using SADABS[13] (T_{max} = 0.74, T_{min} = 0.47). The structure was solved by direct methods. Terbium and oxygen atoms were refined with anisotropic displacement parameters, and carbon atoms with isotropic parameters. Hydrogen atoms of the organic ligands were included but not refined. The final cycle of full-matrix least-squares refinement was based on 3156 observed reflections ($I > 3.00\sigma(I)$) and 227 variables and refined to convergence R_1 = 0.058 (unweighted, based on F)and R_w = 0.065. The maximum and minimum peaks on the final difference Fourier map corresponded to 5.19 and -1.87 e$^-$ Å^{-3}, respectively. Crystallographic data (excluding structure factors) for the structures reported in this paper have been deposited with the Cambridge Crystallographic Data Centre as supplementary publication no. CCDC-119758. Copies of the data can be obtained free of charge on application to CCDC, 12 Union Road, Cambridge CB2 1EZ, UK (fax: (+44) 1223-336-033; e-mail: deposit@ccdc.cam.ac.uk).

[8] Generation of 3- and (3,4)-connected nets from 4-connected nets: M. O'Keeffe, B. G. Hyde, *Crystal Structures I: Patterns and Symmetry*, Mineralogical Society of America, Washington, DC, **1996**, p. 359.

[9] Elemental analysis (%) calcd for $C_8H_4O_7$NTb: Tb(bdc)(NO_3) C 24.95, H 1.05, N 3.64; found: C 25.37, H 1.31, N 3.95. FT-IR (KBr, 2000 – 500 cm^{-1}): $\tilde{\nu}$ = 1630 (m), 1564 (s), 1512 (m), 1387 (vs), 1320 (w), 1163 (w), 1117 (w), 1025 (w), 893 (w), 847 (w), 814 (w), 761 (m), 518 cm^{-1} (m). When this material is exposed to DMF vapor for 1 d, the original product is regenerated. Elemental analysis (%) calcd for the regenerated product $C_{14}H_{18}O_9N_3$Tb: Tb(bdc)$(NO_3)\cdot 2$DMF: C 31.65, H 3.42, N 7.91; found: C 31.40, H 3.44, N 7.88.

  1433-7851/99/3817-2593 $ 17.50+.50/0

[10] A standard solution containing the same guest concentration was periodically checked with the same techniques employed for each experiment. To further show that the alcohol guests were included within the pores rather than on the crystal surface, the GC sample was filtered, washed with toluene, air dried, and then elemental microanalysis was performed to confirm the presence of alcohol.
[11] *SAX Area-Detector Integration Program (SAINT)*, V4.024, Siemens Industrial Automation, Inc., Madison, WI, **1995**.
[12] XPREP, V5.03, is part of the program *SHELXTL Crystal Structure Determination*, Siemens Industrial Automation, Inc., Madison, WI, **1995**.
[13] *Siemens Area Detector ABSorption correction program (SADABS)*, G. Sheldrick, personal communication, **1996**.

Stable Polymer-Bound Iodine Azide**

Andreas Kirschning,* Holger Monenschein, and Carsten Schmeck

Dedicated to Professor Armin de Meijere on the occasion of his 60th birthday

In addition to numerous methods for the syntheses of organic molecules on polymeric supports, there has been a recent upsurge in the interest in the use of polymer-bound reagents in organic chemistry.[1] The intrinsic advantage of this hybrid solid-/solution-phase technique lies in the simple work-up and isolation of the reaction products combined with the flexibility of solution-phase chemistry. Furthermore, these reagents may be used in excess in order to drive the reaction to completion without making the isolation of the products more difficult. Although stoichometric polymer-supported reagents have been employed in organic synthesis for many years, their application to the construction of small molecule libraries is a relative recent phenomenon. This can be ascribed to the fact that the number of readily available reagents of this type is still small. Important developments in this field are polymer-supported reductants,[2] oxidants,[3] solution-phase scavengers,[4] chelating proton donors,[5] carbodimide equivalents,[6] or reagents that are capable of promoting C–C bond-forming reactions.[7] However, polymer-bound reagents for 1,2-cohalogentions[8, 9] of alkenes have not been described so far.[10]

As an extension of our earlier work on ligand-transfer reactions from hypervalent iodine(III) reagents to halides in solution,[11] we initiated a study on the development of the first stable electrophilic polymer-bound reagent that synthetically behaves like iodine azide (**3b**). Since the pioneering work of Hassner et al.[12] azido-iodination of alkene double bonds has become a very useful procedure for introducing a nitrogen functionality into a carbon skeleton. Iodine azide (**3b**) has commonly been generated in situ from sodium azide and iodine chloride in polar solvents.[12, 13] However, its explosive character is regarded to be a major disadvantage.

Our approach to iodine azide (**3b**) is based on the reaction of (diacetoxyiodo)benzene with polystyrene-bound iodide **1** in dichloromethane at room temperature, which presumably afforded polymer-bound di(acetyloxy)iodate(I) (**2**) (Scheme 1).[14, 15] Treatment of **2** with trimethylsilylazide furnished a resin which synthetically acts like immobilized iodine azide (**3b**). However, extensive washing of the resin does not result in deactivation thus we propose that polymer-bound bis(azido)iodate(I) (**3a**) is the active species. Reagent

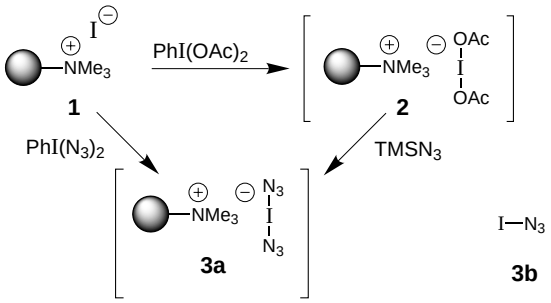

Scheme 1. Preperation of novel polymer-bound iodine azide. TMS = Me_3Si.

3a may also be generated by direct azido transfer after treatment of iodide **1** with (diazidoiodo)benzene. However, as $PhI(N_3)_2$ has to be prepared in situ from (diacetoxyiodo)benzene and trimethylsilylazide efficient azido transfer to **1** is hampered by the presence of trimethylsilyl acetate in solution. The IR spectrum of the new polymer **3a** shows a pair of strong bands at $\tilde{\nu} = 2010$ and 1943 cm^{-1}, which confirm the presence of an azido group. It smoothly promotes azido-iodination of alkenes **4**–**18** to give the *anti* addition product (Table 1).[16] Except for electron-defficient alkenes **5** and **11** and for methylenecyclopropane **17** (Table 1), sensitive β-iodo azides **19**, **21**–**25**, and **27**–**33** are generated in good to excellent yield. They are conveniently purified by filtration and removal of the solvent.[17] The regioselectivity of the 1,2-addition is governed by the more stable intermediate carbenium ion formed after electrophilic attack. Only when alkyl-substituted alkenes **15** and **16** were subjected to the azido-iodination conditions, were small amounts of the *anti*-Markovnikov 1,2-adducts formed. Remarkably, free hydroxy groups in allyl or homoallyl position, such as in alkenes **7**, **13**, and **14**, are tolerated under the conditions employed. Addition to methylenecyclopropane **17** proceeded in a highly regioselective and stereoselective manner to furnish **32**. Rearrangement products which may have originated from the very stable intermediate cyclopropylmethyl cation[18] were not isolated. The relative configuration of **32** was uneqivocally assigned by nuclear Overhauser effect (NOE) experiments (Table 2). Finally, also 1,2-functionalization of carbohydrate-

[*] Dr. A. Kirschning, H. Monenschein
Institut für Organische Chemie der Technische Universität Clausthal
Leibnizstrasse 6, D-38678 Clausthal-Zellerfeld (Germany)
Fax: (+49) 5323-72-2858
E-mail: andreas.kirschning@tu-clausthal.de
Dr. C. Schmeck
Bayer AG, Business Group Pharma PH-R-CR, D-42096 Wuppertal (Germany)

[**] This work was supported by the Fonds der Chemischen Industrie. We thank Bayer AG and particularly Dr. D. Häbich (Wuppertal) for financial and technical support.

  1433-7851/99/3817-2594 $ 17.50+.50/0